A. Zangarini, D. Invernizzi, P. Panizza, M. Lovera
Closed-Loop MIMO Data-Driven Attitude Control Design for a Multirotor UAV
CEAS Aeronautical Journal, In press - Published online 11/06/2020
doi:10.1007/s13272-020-00456-9

CEAS Aeronautical Journal manuscript No.
(will be inserted by the editor)

Closed-loop MIMO data-driven attitude control design for a multirotor UAV

A. Zangarini · D. Invernizzi · P. Panizza · M. Lovera

Received: date / Accepted: date

Abstract In this paper, the problem of tuning the attitude control system of a multirotor Unmanned Aerial Vehicles (UAV) is tackled and a data-driven approach is proposed. With respect to previous work, the data used to tune the controller gains are collected in flight during closed-loop experiments. Furthermore, the simultaneous tuning of roll and pitch attitude control loops is demonstrated, thus paving the way to MIMO data-driven attitude control design. Simulation results confirmed that a MIMO controller allows rejecting undesired coupling effects that affect the performance of a standard decoupled controller usually employed in autopilots for multirotor UAVs. Finally, the results based on experimental work carried out on a quadrotor UAV show that a good level of performance can be achieved in typical operating conditions with the proposed tuning method.

Keywords UAV · Attitude control · Data-driven control

1 Introduction

Small-scale Unmanned Aerial Vehicles (UAVs), and in particular multirotor ones, have been studied extensively in view of the great potential for a large number of applications. For most problems of practical interest, requirements in terms of pointing and positioning performance require a careful tuning of the control laws. While nonlinear control design approaches have been considered in the literature (see, *e.g.*,[1] for a recent survey), for civil applications such as surveillance, mapping, video and photography linear controllers are usually adopted. In these settings, considering also that hover and near-hover operations are representative conditions, cascaded PID laws are usually employed for attitude control thanks to their inherent reliability and ease

A. Zangarini, D. Invernizzi, P. Panizza, M. Lovera
Dipartimento di Scienze e Tecnologie Aerospaziali, Politecnico di Milano
Tel.: +39-02-23993592
Fax: +39-02-23998334
E-mail: marco.lovera@polimi.it

of implementation. As far as controller tuning is concerned, model-based methods suffer from the fact that the mathematical modelling of quadrotors is particularly challenging due to the non-trivial characterization of the aerodynamics and of the actuators and sensors dynamics (see[2]). For this reason data-driven tuning methods, which have been developed in the last two decades in the control community, offer an interesting alternative. These control design tools are especially appealing when *a priori* knowledge about the plant model is limited, when an accurate modeling of the system is too expensive or when fast deployment of the control system is an important requirement, since they allow the direct tuning of the controller parameters from experimental input-output data. Among the data-driven methods available in the literature, a coarse classification can be made between iterative (*e.g.*, the Iterative Feedback Tuning (IFT)[3]) and single-shot (non-iterative) methods (*e.g.*, the Virtual Reference Feedback Tuning (VRFT)[4], the Correlation-Based Tuning (CbT)[5,6]). Recent advances on the VRFT method, which is the approach adopted in this work, can be found *e.g.*, in[7,8,9], while application studies are available, *e.g.*, in[10,11].

Non-iterative methods are particularly attractive for a fast re-tuning of the controller when the plant performance is reduced (*e.g.*, components aging) and/or operating conditions change (*e.g.*, different payloads, environment). Recently ([12]) the VRFT algorithm has been considered to tune the attitude controller parameters of a variable-pitch quadrotor, based on data collected in indoor experiments on a single degree-of-freedom test-bed. The results have shown improvements in the tracking and disturbance rejection capabilities compared to those obtained with a manual tuning. Furthermore, comparable results with respect to a model-based structured H_∞ synthesis ([13]), made data-driven methods a promising tool for this kind of applications. In particular, an extension of VRFT allowing the direct tuning of a cascade controller configuration with a single set of input-output data, following the procedure outlined for the VRFT (see[14]), has been employed. The possibility of tuning the control laws directly from flight-test data has been subsequently explored in[15], as this, among other things, would pave the way to the design and tuning of MIMO (Multiple Input Multiple Output) attitude controllers. Experiments for the tuning of attitude controllers however can be executed safely only in closed-loop conditions. In view of this, in this paper a closed-loop approach to data-driven tuning of the attitude control laws for a multirotor UAV is presented. With respect to previous work, the pitch and roll axes are tuned in a single experiment exploiting a MIMO controller structure using the VRFT method proposed in[16]. Indeed, while the attitude motion of quadrotors can be approximated by three independent equations along each axis in near hovering conditions, a decoupled controller may yield not so satisfactory performance in practice due to unavoidable inertial couplings arising from a non perfect knowledge of principal axes frame and nonlinear effects. The achievable performance is illustrated by means of experimental results obtained on a small-scale quadrotor.

The paper is organized as follows. The data-driven framework is presented in Section 2. In Section 3 the considered quadrotor platform and its controller architecture are introduced in detail. Finally, simulation and experimental results are presented and discussed in Section 4.1 and 4.2 respectively.

2 Data-driven control law design

2.1 VRFT with open-loop data

Consider a linear time-invariant discrete-time system $P(z)$, where z denotes the forward time-shift unit (*i.e.*, $zx(t) = x(t+1)$), a parametrized controller class $\mathscr{C}(\theta) = \{C(z,\theta), \theta \in \mathbb{R}^n\}$, and a given target closed-loop behaviour $M(z)$. The control aim of data-driven methods is the minimization of the weighted $\mathscr{L}_2$-norm of the mismatch between $M(z)$ and the actual closed-loop system:

$$J_{MR}(\theta) = \left\| \left(\frac{P(z)C(z,\theta)}{1+P(z)C(z,\theta)} - M(z) \right) W(z) \right\|_2^2, \tag{1}$$

where $W(z)$ is a weighting function chosen by the user. In data-driven approaches the model-reference problem (1) is solved with limited knowledge of the system and using only a set of available measurements $d_N = \{u(t), y(t)\}_{t=1,\dots,N}$, where N is the length of the data-set and u, y are the input and output to the plant $P(z)$, respectively.

The main idea of VRFT can be described as follows. Consider the reference signal $r(t)$ that would feed the system in closed-loop operation when the closed-loop model is $M(z)$ and the output is the measured $y(t)$. Such a signal is called *virtual reference* and is such that $y(t) = M(z)r(t)$. A good controller (making the closed-loop as close as possible to $M(z)$) is then the one that produces the input sequence of the experiment $u(t)$ when it is fed by the error signal $e(t) = r(t) - y(t)$.

Formally, the cost criterion minimized by the VRFT algorithm is the following:

$$J_{VR}^N(\theta) = \frac{1}{N}\sum_{t=1}^{N} \left(u_L(t) - C(z,\theta)e_L(t)\right)^2, \tag{2}$$

where $u_L(t)$ and $e_L(t)$ are suitably filtered versions of $u(t)$ and $e(t)$. The filter $L(z)$ is chosen such that the cost function (2) is a local approximation of the criterion (1) in the neighborhood of the minimum point[4].

Remark 1 Both VRFT and CbT have been extended to deal with multiple nested loops architectures in[14,17]. Consider the cascade control scheme in Figure 1, given two reference models $M_i(z)$ and $M_o(z)$, for the inner loop and the outer loop respectively, and consider two families of linear proper controllers $\mathscr{C}_i(\theta_i) = \{C_i(z,\theta_i)\ ,\ \theta_i \in R_i^n\}$ and $\mathscr{C}_o(\theta_o) = \{C_o(z,\theta_o)\ ,\ \theta_o \in R_o^n\}$ and the set of data $D_N = \{u(t), y_i(t), y_o(t)\}_{t=1,\dots,N}$ being $u(t)$ the control variable, $y_i(t)$ the output of the inner loop, $y_o(t)$ the output of the outer loop. The inner controller can be tuned by applying VRFT or CbT while for the outer controller the approach needs to be different, as the input of the system to control is the reference $r_i(t)$, that is not available in the dataset, since measurements are collected during open-loop operation. Nevertheless, the reference signal $r_i(t)$ can be derived as follows: once $C_i(z,\theta_i)$ is fixed, the input of the inner loop can be calculated as $r_i(t) = e_i(t) + y_i(t)$, where the tracking error comes from the result of the inner design: $e_i(t) = C_i^{-1}(z,\theta_i)u(t)$. With such a choice, $r_i(t)$ is exactly the signal that would feed the inner loop in closed-loop working conditions when the output is $y_i(t)$. Then, the outer controller can be easily found by using the set of I/O data $D_N^o = \{r_i(t), y_o(t)\}_{t=1,\dots,N}$.

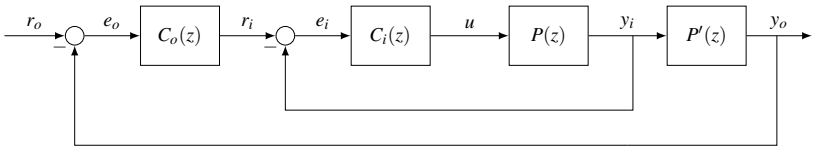

Fig. 1: Cascade control scheme with two nested loops.

Remark 2 Since VRFT exploits a PEM (Prediction Error Method) identification procedure to tune the controller, it has to deal with the problem related to these class of methods. In particular, suppose that the output of the plant is affected by an additive noise $v(t)$ (see Figure 2)

$$\tilde{y}(t) = P(z)u(t) + v(t),$$

with the assumption that $u(t)$ and $v(t)$ are uncorrelated. In this case the PEM procedure is not adequate for this problem because the input of the controller is affected by the noise $v(t)$ and this results in a biased parameter vector estimate. As described in[4], an instrumental variable method can be employed to counteract the effect of noise. The instrumental variable can be built in different ways and it must be correlated with the regression variable and uncorrelated with the noise $v(t)$. To satisfy these requirements, the instrumental variable can be developed by exploiting repeated experiments or by plant identification[4]. In some situations a second experiment with the same input signal can not be performed. Thus, a way to build the instrumental variable passes through the identification of the plant in order to get a model $\hat{P}(z)$. The model can be exploited to build the noiseless output as:

$$\hat{y}(t) = \hat{P}(z)u(t) \tag{3}$$

and the instrumental variable is

$$\zeta(t) = \beta(z)L(z)\left(M(z)^{-1} - 1\right)\hat{y}(t) \tag{4}$$

where $\beta(z)$ is defined such that $C(z,\theta) = \beta^T(z)\theta$. This approach guarantees a consistent estimate but its variance depends on the quality of the model $\hat{P}(z)$. Furthermore, the plant identification procedure clashes with the data-driven idea of the VRFT method. Nevertheless the reader should notice that $\hat{P}(z)$ is not directly involved in the design of the controller but it is employed only in the creation of the instrumental variable. Once the instrumental variable is selected, it can be used to solve the problem in (2) and the optimal solution is[4]:

$$\hat{\theta}_N^{IV} = \left[\sum_{t=1}^{N} \zeta(t)\varphi_L^T(t)\right]^{-1} \sum_{t=1}^{N} \zeta(t)u_L(t). \tag{5}$$

where $\psi_L(t) = \beta(z)e_L(t)$ is a regressor vector.

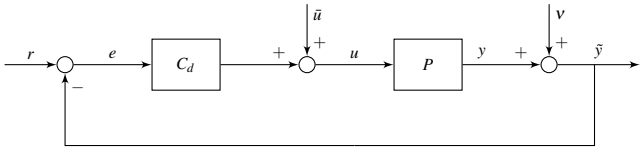

Fig. 2: VRFT experiment in closed-loop operation.

2.2 VRFT with closed-loop data

If the test to collect data is performed in flight, then for safety reasons the data must be collected in closed-loop, allowing the user to control the system also during the experiment. Furthermore, closed-loop tests allow to perform the experiment to collect the data without exploiting a test-bed and without modifying the system, thus significantly simplifying the tuning process.

As illustrated in Figure 2, the excitation input $\bar{u}$ is added to the output of the controller $C_d(z)$. $C_d(z)$ is a stabilising controller adopted to carry out the in-flight test. The user can act on the set-point r to control the behaviour of the system also during the experiment.

The standard VRFT method cannot be applied to obtain a new controller exploiting the measurements $d_N = \{u(t), \tilde{y}(t)\}_{t=1,\dots,N}$: specific problems arise when the instrumental variable is constructed because u and the noise v are correlated. Indeed, the user cannot directly act on the input of the plant as in the standard VRFT, but it can operate on the setpoint r and on the excitation input $\bar{u}$, and the input of the plant is now affected by this action:

$$u(t) = \frac{1}{1+C_d(z)P(z)}\bar{u}(t) + \frac{C_d(z)}{1+C_d(z)P(z)}\left(r(t) - v(t)\right). \tag{6}$$

For the sake of simplicity, the assumption that the user does not provide a setpoint during the experiment can be made ($r(t) = 0,\ \forall\, t$) and (6) can be rewritten as:

$$u(t) = \frac{1}{1+C_d(z)P(z)}\bar{u}(t) - \frac{C_d(z)}{1+C_d(z)P(z)}v(t). \tag{7}$$

Using (7) to build the instrumental variable (4) leads to a biased controller parameter vector since the instrumental variable is no longer uncorrelated with the noise $v(t)$. Indeed, if one were to substitute (7) in equation (3), he would get

$$\hat{y}(t) = \hat{P}(z)\left(\frac{1}{1+C_d(z)P(z)}\bar{u}(t) - \frac{C_d(z)}{1+C_d(z)P(z)}v(t)\right).$$

Then, the instrumental variable (4) would be given by

$$\begin{aligned}\zeta(t) &= \beta(z)L(z)\left(M(z)^{-1}-1\right)\hat{y}(t)\\ &= \beta(z)L(z)\left(M(z)^{-1}-1\right)\\ &\quad \hat{P}(z)\left(\frac{1}{1+C_d(z)P(z)}\bar{u}(t) - \frac{C_d(z)}{1+C_d(z)P(z)}v(t)\right).\end{aligned}$$

The previous equation clearly shows the correlation between $\zeta(t)$ and $v(t)$. To solve this problem a different instrumental variable must be chosen, to ensure correlation with the regression variable and incorrelation with the noise. A detailed overview on the choice of the instrumental variable can be found in[15]. In this work we will employ the following instrumental variable:

$$\zeta(t) = \beta(z)L(z)\left(M(z)^{-1} - 1\right)\hat{y}_{\bar{u}}^{CL}(t) \tag{8}$$

where

$$\hat{y}_{\bar{u}}^{CL}(t) = \frac{\hat{P}(z)}{1 + C_d(z)\hat{P}(z)}\bar{u}(t),$$

which is clearly uncorrelated with the noise. Note that if the instrumental variable is built as in (8) the initial controller $C_d(z)$ must be known. In the next Section we will present an alternative formulation of the VRFT method which naturally extends to MIMO systems and requires less information, notably, no plant model is needed to built the instrumental variable and the initial controller parameters should not be known.

2.3 Multivariable extension

The VRFT algorithm can be extended to the multivariable case, where the initial formulation is the same, but an additional step is introduced. In particular, a different instrumental variable method is employed, the extended instrumental variable (EIV), which is easily implemented for multivariable problems[18] and does not require neither the identified model to counteract the effect of noise. In this section we follow closely the presentation of[16], to which we refer the interested reader for further details. Different multivariable approaches in the VRFT framework can be found in[19,20].

The discrete MIMO LTI problem is formulated in terms of a MIMO linear time-invariant discrete time model $P(z) \in \mathbb{R}^{n_y \times n_u}$, a linearly parametrized controller $C(z,\theta) \in \mathbb{R}^{n_u \times n_y}$ where $u \in \mathbb{R}^{n_u}$, $y, r \in \mathbb{R}^{n_y}$. The model reference problem is then formulated with respect to the input complementary sensitivity $T(z) \in \mathbb{R}^{n_y \times n_y}$, thus the reference model is such that $M(z) \in \mathbb{R}^{n_y \times n_y}$.

A convex approximation of (1) for the multivariable case, namely,

$$\tilde{J}_{MR}(\theta) = \|M(z) - (I - M(z))P(z)\beta^T(z)\theta\|_2^2, \tag{9}$$

can be obtained by making the following assumptions:

1. the desired sensitivity function $S(z) = I - M(z)$ is close to the actual closed-loop sensitivity function for $\theta = \hat{\theta}$ (the minimizer of (1)) , *i.e.*, $(I + P(z)C(z,\hat{\theta}))^{-1} \approx I - M(z)$;
2. the controller family $C(z,\theta)$ can be linearly parametrized with the vectors of parameters $\theta \in \mathbb{R}^n$, such that $\mathscr{C}(\theta) = \left\{C(z,\theta) = \beta^T(z)\theta\right\}$.

By comparing the frequency-wise counterpart of the virtual reference cost function, defined here as

$$J_{VR}^{N}(\theta) = \frac{1}{N}\sum_{t=1}^{N}\left(u_{L_u}(t) - C(z,\theta)e_{L_e}(t)\right)^2, \tag{10}$$

where $u_{L_u}(t) = L_u u(t)$, $e_{L_e} = L_e(M^{-1} - I)PL_y u(t)$, and the convex approximation of the model reference one in Equation (9), the filters which make them equivalent can be defined as:

$$L_u(z) = M(z)\Phi_{uu}^{-1/2}(z), \quad L_e = C^{-1}(z,\theta)M(z), \quad L_y = C(z,\theta)\Phi_{uu}^{-1/2}(z), \tag{11}$$

where Φ_{uu} is the power spectral density of the input u. These filters however require the knowledge of the controller, turning the minimization of (10) into a nonlinear optimization problem. Instead, by choosing suboptimal filters[1] as:

$$L_u(z) = L_e(z) = L(z) = M(z), \quad L_y(z) = I, \tag{12}$$

the cost function (10) becomes linear in the parameter vector, and the frequency-wise version of the asymptotic value of J_{VR}^{N} can be read as the frequency-wise convex approximation of

$$\bar{J}_{MR}(\theta) = \|M(z) - (I + C(z,\theta)P(z))^{-1}C(z,\theta)P(z)\Phi_{uu}^{1/2}\|_2^2. \tag{13}$$

Remark 3 The main difference between the suboptimal filters and the optimal ones is that $C(z,\theta)$ is chosen in (13) such as to make the input complementary sensitivity function as close as possible to $M(z)$. Nonetheless, good matching results will be observed in practice (see Section 4.2) even if the desired behavior is formulated via output complementary sensitivity function, as noted also in[16]. An asymptotically exact solution which guarantees that the desired closed-loop dynamics is matched when the number of data tends to infinity can be found in[21].

Without loss of generality, a MIMO FIR structure with integral action will be used. The n-th order control law is then defined as:

$$u(t) = u(t-1) + \sum_{i=0}^{n} B_i e(t-i) \tag{14}$$

$$= u(t-1) + B_0 e(t) + B_1 e(t-1) + \cdots + B_n e(t-n), \tag{15}$$

where $B_i \in \mathbb{R}^{n_u \times n_y}, i = 1,\ldots,n$. The linearly parametrized PID class can be obtained by exploiting the properties of the Kronecker product, denoted with $\otimes$, as follows:

$$u(t) = u(t-1) + \sum_{i=0}^{n} B_i e(t-i) = u(t-1) + \varphi^T(t)\theta \tag{16}$$

$$\begin{aligned}\sum_{i=0}^{n} B_i e(t-i) &= \left[e^T(t)\otimes I, \cdots, e^T(t-n)\otimes I\right]\ \mathrm{vec}\left([B_0,\cdots,B_n]\right)\\ &= \varphi^T(t)\theta,\end{aligned} \tag{17}$$

[1] It is noted that the filters for the MIMO extension differ from the ones derived for the SISO problem, as obtained in[4]. This is due to Assumption 1 being used at the beginning of the derivation, obtaining the filter for the convex model reference problem instead of deriving the optimal filter first for the original model reference problem. The filters are optimal in case of SISO systems, see Section 3 of[16].

where:

$$\theta = \mathrm{vec}\left([B_0, \cdots B_n]\right) \tag{18}$$

$$\varphi(t) = \left[e^T(t) \otimes I, \cdots, e^T(t-n) \otimes I\right]^T. \tag{19}$$

The definition of the regressor φ and the parameter vector $\theta \in \mathbb{R}^{n_\theta}, n_\theta = n \times n_u \times n_y$ in Equation (16) can be further manipulated obtaining:

$$u(t) = \frac{1}{1-z^{-1}}\varphi^T(t)\theta = \frac{z}{z-1}\varphi^T(t)\theta = \varphi_F^T(t)\theta. \tag{20}$$

Following[16], an Extended Instrumental Variable (EIV) is introduced, which is obtained by taking a window of length $\pm\ell$ of the input:

$$\zeta^e(t) = \begin{Bmatrix} u(t+\ell) \\ \vdots \\ u(t-\ell) \end{Bmatrix}. \tag{21}$$

The EIV variable can now be used to define a decorrelation cost function, as described in[16]:

$$J_D^N(\theta) = (r - R\theta)^T \hat{W}^{-1}(r - R\theta) \tag{22}$$

$$R = \frac{1}{N}\sum_{t=1}^{N} \zeta_L^e(t) \otimes \varphi_L(t) \tag{23}$$

$$r = \frac{1}{N}\sum_{t=1}^{N} \zeta_L^e(t) \otimes u_L(t), \tag{24}$$

where φ_L is the regressor defined from signals filtered with (12), $\zeta_L^e(t) = L\zeta^e$ and $\hat{W}$ is a positive semi-definite weight, optimally a consistent estimate of the residual covariance matrix

$$\bar{W} = \mathbb{E}\left[(r - R\theta)(r - R\theta)^T\right]. \tag{25}$$

The decorrelation function in the absence of noise, for large windows ℓ, leads asymptotically to $R\theta - r = 0$. Thus, the minima of the decorrelation cost function (22) are equivalent to the minima of the virtual reference cost function (2), and are given by:

$$\hat{\theta} = \arg\min_{\theta} J_D(\theta) = \left(R^T W^{-1} R\right)^{-1}\left(R^T W^{-1} r\right). \tag{26}$$

The length of the window for the EIV method represents a tuning knob of the algorithm, however an arbitrarily large number can be used.

Remark 4 As is well-known in the literature about model reference tuning methods, the choice of the reference model heavily influences the result of the tuning algorithms. In particular, stability of the closed-loop system for a given reference model is not a priori guaranteed by all algorithms[5]. Different controller structures can lead

to quite different performance since the resulting closed-loop systems can approximate the reference model with a different bias. Issues such as non-minimum phase plants, including the presence of time delays, can become critical[7]. Defining reference models in the data-driven framework is not straightforward, as this would require knowledge of the system which data-driven methods aim to eliminate. However, keeping in mind that the reference model expresses the desired dynamics for the complementary sensitivity function of the closed-loop system, it is usually sufficient to have some knowledge of the dominant dynamics of the system , often expressed as a second-order model. In such a case the desired crossover frequency can be defined, and an approximation of the system damping ratio can be set. These simple reference models can be used when the required performance is conservative or as a first iteration, such that the collected data is sufficiently informative over the bandwidth of interest. However, when better performance is required, the reference model can be enhanced by suitably introducing additional poles and zeros. The presence of time delays can also be determined (using data analysis methods, such as correlation analysis, on the collected data set) to relax the requirements on the control effort, making it more compatible with the dataset. Therefore, data-driven model reference methods such as the ones exploited in this work find their best use in case of fast re-tuning of the controller when the performance of the closed-loop system is reduced due to aging or when the operating conditions change. For additional details about the choice of appropriate reference model see[22,23].

3 Multirotor platform and control architectures

The considered multirotor platform, called ADAM-0 (see Figure 3), is a fixed-pitch quadrotor with the following characteristics:

- Take-Off Weight (TOW): approximately 1450 grams;
- Battery: 4S Li-Po 4000 mAh;
- Flight time: 12 minutes;
- Frame dimensions (footprint): 500 mm (excluding rotors).

Concerning the baseline control architecture, the ADAM-0 platform adopts an attitude control scheme based on identical decoupled cascaded PID loops for the pitch, roll and yaw axes, running at 250 Hz. For instance, focusing on the pitch axis, the outer loop (measured angle ϑ, set-point ϑ^o) is a P controller, while the inner controller is a complete PID that computes the control torque M. More specifically, the derivative action of the inner loop is computed starting from the pitch rate q and not from the pitch angular rate error. Without loss of generality, in this work we will focus on the pitch and roll angle alone: the default parameters for the pitch and roll axis of the controller are shown in Table 1, which will be used for the experiment that follow.

The decoupled architecture is justified by the fact that if the body axes are principal axes of inertia, then when the quadrotor is in near-hovering conditions the Degree of Freedoms (DoFs) could be assumed decoupled. Note, in passing, that the symmet-

Fig. 3: The ADAM-0 UAV.

Table 1: ADAM-0: default controller parameters.

K_P^O	K_P^I	K_I^I	K_D^I
$\begin{bmatrix} 6.5 & 0 \\ 0 & 6.5 \end{bmatrix}$	$\begin{bmatrix} 0.15 & 0 \\ 0 & 0.15 \end{bmatrix}$	$\begin{bmatrix} 0.05 & 0 \\ 0 & 0.05 \end{bmatrix}$	$\begin{bmatrix} 0.003 & 0 \\ 0 & 0.003 \end{bmatrix}$

ric configuration of multirotors [2] allows one to easily identify a set of principle axes of inertia. Hence, the attitude control problem is reduced to a set of three separate problems for, respectively, the pitch, roll and yaw axes. This, in turn, implies that the controllers for each axis can be tuned independently, for instance by exploiting the VRFT method outlined in Section 2.2. In practice, however, the system does not have an exactly decoupled attitude dynamics and a Multiple Input Multiple Output (MIMO) controller should be considered to enforce a desirable decoupled behavior

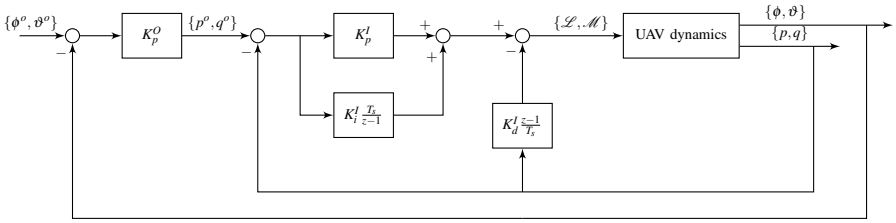

Fig. 4: Block diagram of the control system.

[2] Inspecting Figure 3, there are two planes of symmetry containing the axis orthogonal to the rotors, one having the other two axes aligned with the axes of the arms (+ configuration) and one having the other two axes making 45 deg with respect to the axes of the arms (x configuration))

among the axes and improve performance. In this case, full 2×2 gain matrices must be employed in which the diagonal terms affect the control action over the same axis of the measurement, for instance, pitch rate error leading to a pitch moment. Instead the off-diagonal terms lead to control action on the other channel: the ij-th $(i \neq j)$ component of the controller gives an effect on input i for an error on component j. These terms represent the decoupling action of the MIMO controller. A diagonal matrix is consequently equivalent to a set of two decoupled controllers. The multivariable version of the Virtual Reference Feedback Tuning (VRFT) (see Section 2) will be employed in the next sections to tune the parameters of the considered MIMO controller. To this aim, note that the overall control structure can be converted into the regressor form in equation (16) in a straightforward step, resulting in:

$$\begin{aligned} u(t) &= u(t-1) + \sum_{i=0}^{n_e} B_i e(t-i) + \sum_{j=0}^{n_y} B_j y(t-j) + \sum_{m=0}^{n_r} B_m r(t-m) \\ &= u(t-1) + \varphi^T(t)\theta \end{aligned} \tag{27}$$

where $u(t) = [\mathscr{L}(t)\, \mathscr{M}(t)]^T$ and B_i are suitable matrices collecting the control parameters in the diagonal matrices K_P^O, K_P^I, K_I^I and K_D^I.

4 Results

4.1 Simulation results

A complete Simulink ADAM-0 nonlinear simulator has been used to validate the results of the algorithm. The simulator is able to replicate the attitude dynamics under feedback control on all axes. An artificial inertial coupling has been introduced, where the off-diagonal terms represent 10% of the diagonal terms. These terms will introduce gyroscopic effects since the pitch and roll axis are no longer principal axes of inertia. Noise has been introduced in the system, modeled as white noise with a standard deviation obtained from hovering endurance tests to account for the uncertainty of the state estimates.

Simulation data is collected in closed-loop in order to create the input and output dataset required for the VRFT algorithm. Two Pseudo Random Binary Sequence (PRBS) excitation signals, one for the pitching moment and one for the rolling moment, are applied consecutively. The input $\bar{u}(t) = \left[\bar{\mathscr{L}}\ \bar{\mathscr{M}}\right]^T$ is injected in the system as shown in Figure 2. The two signals are different but they share the same PRBS parameters (signal amplitude and min/max switching interval). In this case, for each axis, a total excitation time of 20s has been used, with a maximum excitation bandwidth of $50\text{rad}/\text{s}$ and an amplitude of 0.15. The latter is a non-dimensional amplitude, referred to the maximum moment that can be applied. The amplitude of the excitation signal has been selected in order to achieve a good signal-to-noise ratio without inducing nonlinear effect that would undermine the assumption behind the VRFT methods outlined in Section 2.

As illustrated in Section 2.2, an initial controller $C_d(z)$ that stabilizes the system must be available, with parameters collected in Table 1.

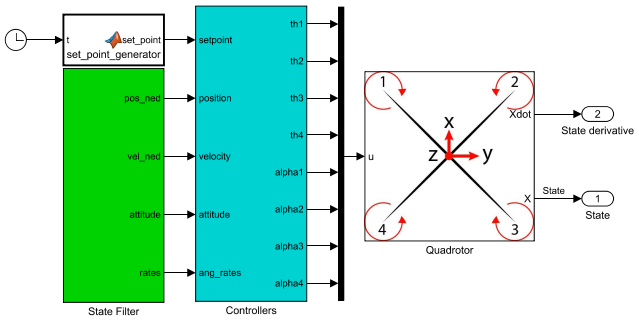

Fig. 5: ADAM-0 *Simulink* model.

Reference models

For both the pitch and roll inner loops, the reference model is a second order model, with a desired bandwidth and damping ratio of 20rad/s and 0.4 respectively:

$$M_i(z) = \frac{0.003131z + 0.003065}{z^2 - 1.932z + 0.9380}.$$

In this specific case no filtering action was needed, thus the weighting function has been defined as $W_i(z) = I$. Therefore, considering the MIMO case the reference models are 2×2 matrices of transfer functions, with the transfer function $M_i(z)$ on the main diagonal and zeros on the secondary diagonal, requiring full decoupling.

Similarly, requirements have been set for the outer loop, once again a second order model, and a slower response. The desired bandwidth is 10rad/s with a damping ratio of 0.7:

$$M_o(z) = \frac{0.0007852z + 0.0007706}{z^2 - 1.9440z + 0.9455}.$$

Controller tunings and comparison

Results from the SISO algorithm applied to both pitch and roll data are then compared to the full MIMO formulation shown in Section 2.3, for the given set of reference models for the inner and outer dynamics. The resulting parameters of both algorithms are illustrated in Table 2. It is shown that the diagonal terms are almost the same. The gains of the outer loop P controller feature an almost identical term on the diagonal, and the outer diagonal terms which are smaller by two orders of magnitude, which is reasonable in view of the small expected cross-couplings between the two axes (see the discussion in Section)

In order to compare the results, a doublet benchmark has been considered, that is a quick consecutive variation of the attitude that has a zero mean. The doublet period $T = 0.42$s and amplitude $A = 22.5$ deg is held constant among the different tests. The simulated pitch doublet is shown in Figure 6, where it is highlighted that the full MIMO controller is able to significantly reduce the coupling effects. It can be seen that while the control effort is comparable, a better attitude tracking is achieved.

Table 2: ADAM-0: optimal controller parameters for outer and inner controllers considering the VRFT method with closed-loop simulation data.

	K_P^O	K_P^I	K_I^I	K_D^I
MIMO	$\begin{bmatrix} 5.2090 & 0.0104 \\ 0.0114 & 5.1874 \end{bmatrix}$	$\begin{bmatrix} 0.1464 & 0.0094 \\ 0.0094 & 0.1275 \end{bmatrix}$	$\begin{bmatrix} 0.2630 & 0.0038 \\ 0.0038 & 0.2555 \end{bmatrix}$	$\begin{bmatrix} 0.0005 & 0 \\ 0 & 0.0004 \end{bmatrix}$
SISO	$\begin{bmatrix} 4.6650 & 0 \\ 0 & 4.6772 \end{bmatrix}$	$\begin{bmatrix} 0.1490 & 0 \\ 0 & 0.1300 \end{bmatrix}$	$\begin{bmatrix} 0.1765 & 0 \\ 0 & 0.1807 \end{bmatrix}$	$\begin{bmatrix} 0.0001 & 0 \\ 0 & 0.0001 \end{bmatrix}$

4.2 Experimental results

The experimental data is collected in the same way as presented for the simulation result. The default controller parameters are used as the initial regulator, illustrated in Table 1.

Figure 7a and Figure 7b show the involved signals in the data-driven tuning procedure. These signals share the same specifications of the simulated experiment in Section 4.1. For the sake of clarity, the signals are represented in two figures but were collected sequentially during the same flight.

Reference models

As seen in Section 4.1, the chosen reference models are second order models with the addition of a delay. The choice of the reference model in data-driven methods can affect the stability of the feedback system, thus it might need adjustments between tests and lead to slightly different results. In this case, the reference model chosen for the SISO algorithm is different from the one used for the simulation and MIMO formulation.

Table 3: Model references for the inner and outer loops used for the experiments.

		ω [rad/s]	ζ	Delay
MIMO	Inner loop	18	0.3	1
	Outer loop	10	0.8	1
SISO	Inner loop	20	0.4	3
	Outer loop	10	0.7	3

Controller tunings and comparison

The benchmark for the performance comparison is a doublet, with period $T = 0.45$s and amplitude $A = 40$deg, similarly to the simulation section. Exploiting the reference models and closed-loop experimental data, the VRFT method leads to the parameter values reported in Table 4. Note again that the secondary diagonal of the parameters in Table 4 is always one or more orders of magnitude smaller than the primary terms.

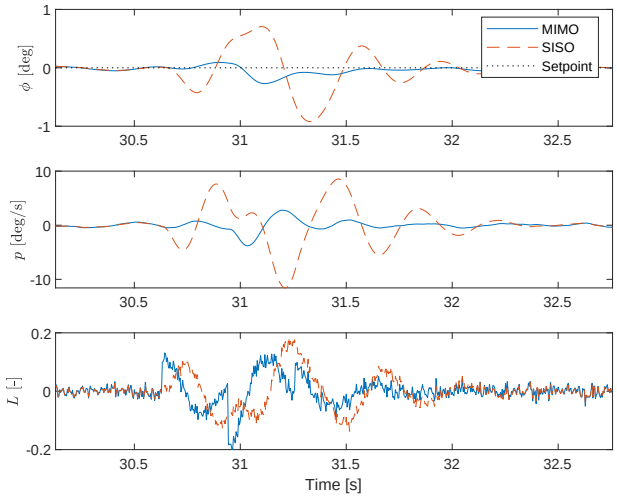

(a) Roll response

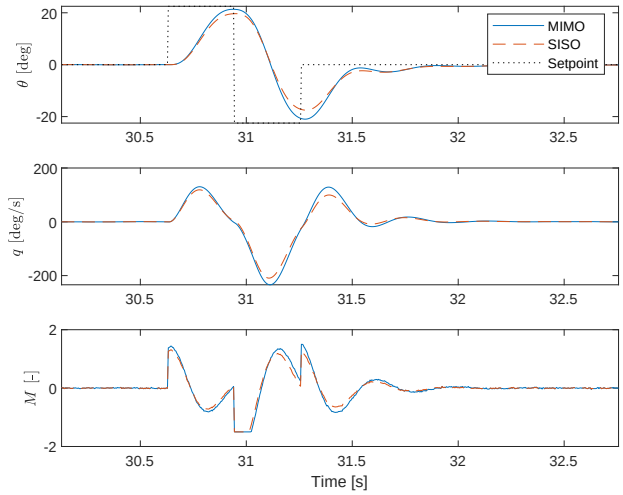

(b) Pitch response

Fig. 6: Simulation of pitch attitude doublet

Since the doublet experiment requires the position and velocity outer feedback loops to be disabled, experiments have been carried out manually by a pilot, leading to difficulties in replicating the exact input and conditions. Preliminary tests are shown in Figures 8 and 9, where the roll doublet response shows a coupling, which in both cases is very limited, as expected. Inspecting the time responses, the pitch angle variations are about $\pm$ 3 deg, however they are smoother for the MIMO solu-

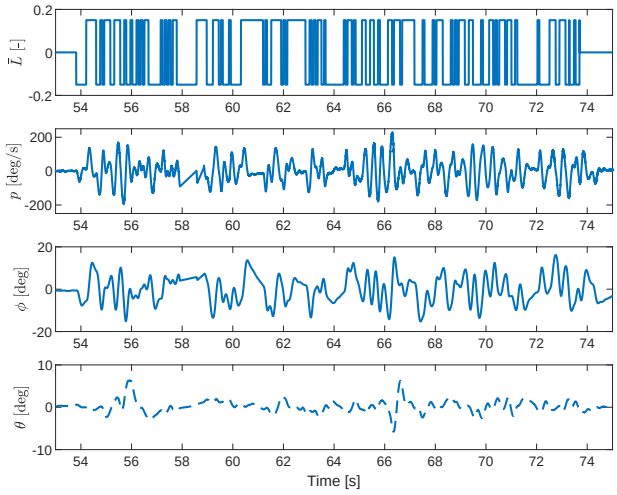

(a) Roll excitation.

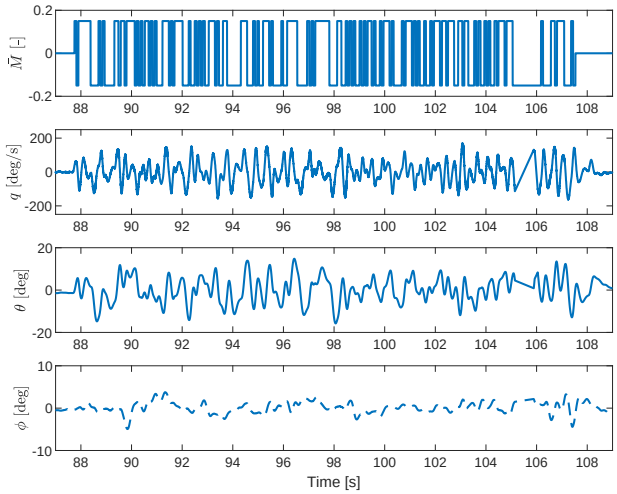

(b) Pitch excitation

Fig. 7: ADAM-0: closed-loop experimental dataset used by MIMO data-driven method.

Table 4: ADAM-0: optimal controller parameters for outer and inner controllers considering the VRFT method with closed-loop experimental data.

	K_P^O	K_P^I	K_I^I	K_D^I
MIMO	$\begin{bmatrix} 4.4484 & -0.1287 \\ 0.2364 & 5.2220 \end{bmatrix}$	$\begin{bmatrix} 0.1187 & -0.0004 \\ 0.0044 & 0.1252 \end{bmatrix}$	$\begin{bmatrix} 0.1749 & 0.0023 \\ 0.0090 & 0.1164 \end{bmatrix}$	$\begin{bmatrix} 0.0007 & 0.0001 \\ 0 & 0.0011 \end{bmatrix}$
SISO	$\begin{bmatrix} 4.2505 & 0 \\ 0 & 4.2061 \end{bmatrix}$	$\begin{bmatrix} 0.1381 & 0 \\ 0 & 0.1495 \end{bmatrix}$	$\begin{bmatrix} 0.1039 & 0 \\ 0 & 0.3039 \end{bmatrix}$	$\begin{bmatrix} 0.0015 & 0 \\ 0 & 0.0027 \end{bmatrix}$

tion. Note that the regulator obtained from the MIMO algorithm leads to a quicker response. The MIMO controller also features a quick suppression of the oscillations in the pitch rate loop, which is able to follow the rate setpoint given from the attitude feedback loop. Finally, the control effort on the pitch axis is reduced with respect to the SISO controller.

To evaluate the performance on the roll axis in a more systematic manner, the reference models have also been simulated for the measured attitude setpoint and compared to the responses of the roll rate and roll angle, see Figure 10. Furthermore, two cost functions have been defined in order to compare the results, one for the setpoint tracking error and one for the model tracking error, for which a qualitative result, based on the time domain response, has been described. Specifically, the cost functions are:

$$J_M = \frac{1}{N} \sum_{k=k_0}^{k_0+N} (\phi(k) - M_o(z)\phi^o(k))^2 \tag{28}$$

$$J_r = \frac{1}{N} \sum_{k=k_0}^{k_0+N} (\phi(k) - \phi^o(k))^2 \tag{29}$$

where k_0 indicates the starting point of the doublet, while N is the number of samples of the doublet and $M_o(z)$ is the reference model for the outer loops. The subscript M indicates the model tracking cost, while the subscript r indicates the setpoint tracking cost. The results are collected in Table 5: as can be seen from the table, and consistently with Figure 10, the MIMO controller performs better than the SISO one both in terms of setpoint and model tracking.

Table 5: ADAM-0: roll performance cost functions from experimental data.

	$\mathbf{J_{M,o}}$	$\mathbf{J_{r,o}}$
MIMO	0.0033	0.1612
SISO	0.0122	0.2645

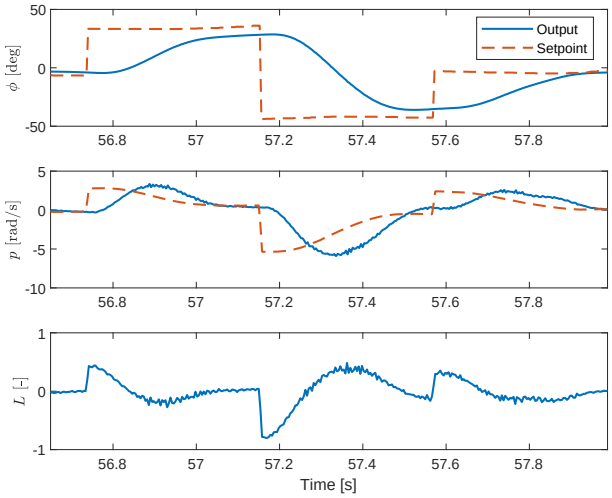

(a) Roll response

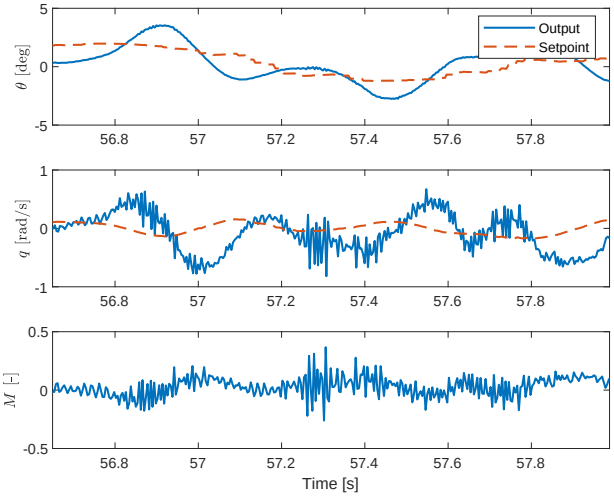

(b) Pitch response

Fig. 8: ADAM-0: Roll doublet experiment with SISO method parameters.

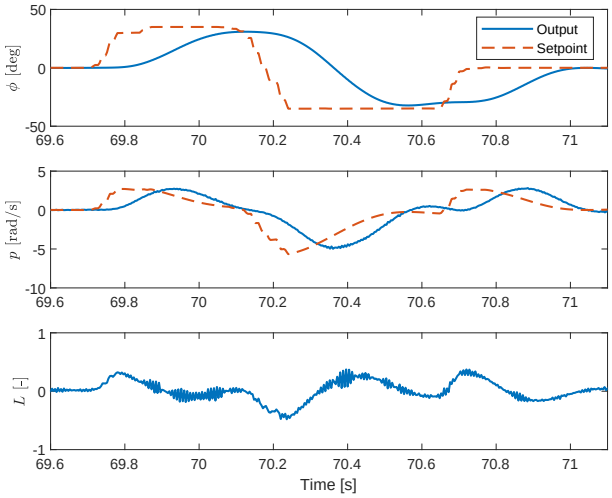

(a) Roll response

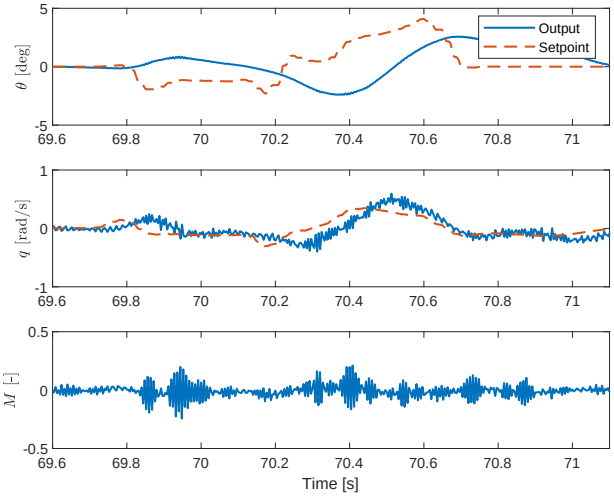

(b) Pitch response

Fig. 9: ADAM-0: Roll doublet experiment with MIMO method parameters.

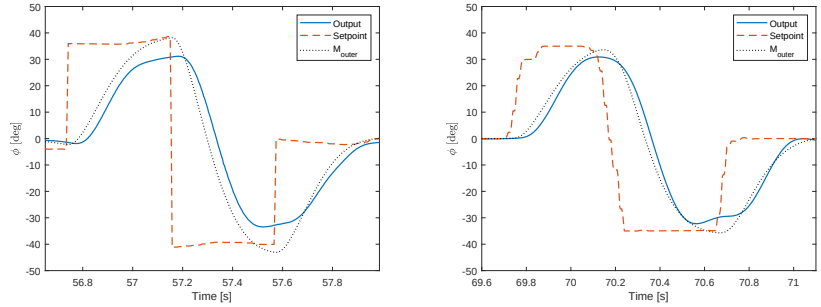

(a) SISO roll angle.

(b) MIMO roll angle.

Fig. 10: ADAM-0: Roll axis performance of the nominal configuration.

5 Conclusions

The problem of data-driven design of the attitude control law for a multirotor UAV has been considered. The VRFT method has been extended to consider a more general class of controllers and by allowing the closed-loop execution of data-collection experiments on the system. Experimental results show that the in-flight tests can be conducted in a safe way and that a satisfactory level of performance can be achieved by using a 20 seconds data sets.

It is highlighted that the MIMO formulation of the problem allows to reduce the effects of coupling that can arise for aggressive manoeuvres, such as the ones featured in the experiments, even for the case of seemingly symmetrical builds. These couplings typically arise from a number of dynamic and aerodynamic effects which are difficult to model, thus all situations leading to a nonlinear behaviour. These effects make this class of synthesis methods very appealing, since almost no assumptions on the system are made.

As with other data-driven methods, no stability constraint is enforced on the algorithm, making the solution of the method reliant on the choice of a suitable reference model. The main advantages over the classic SISO formulation are that the instrumental variable parameters (model order and past/future windowing, see [15]) are not needed, thereby reducing the number of tuning variables. Furthermore, for one of the possible choice of instrumental variable for the classic SISO algorithm, the initial controller must be known, while in the MIMO formulation it is no longer necessary. Finally, this method allows a more general approach to the problem, removing the hypothesis of symmetric configurations and decoupled dynamics.

References

1. R. Mahony, V. Kumar, and P. Corke. Multirotor Aerial Vehicles: Modeling, Estimation and Control of Quadrotor. *IEEE Robotics & Automation Magazine*, 19(3):20–32, 2012.
2. F. Riccardi, P. Panizza, and M. Lovera. Identification of the attitude dynamics for a variable-pitch quadrotor UAV. In *40th European Rotorcraft Forum, Southampton, UK*, pages 1–9, 2014.
3. H. Hjalmarsson, M. Gevers, S. Gunnarsson, and O. Lequin. Iterative feedback tuning: theory and applications. *IEEE Control Systems*, 18(4):26–41, 1998.
4. M.C. Campi, A. Lecchini, and S.M. Savaresi. Virtual reference feedback tuning: a direct method for the design of feedback controllers. *Automatica*, 38(8):1337–1346, 2002.
5. K. Van Heusden, A. Karimi, and D. Bonvin. Data-driven model reference control with asymptotically guaranteed stability. *International Journal of Adaptive Control and Signal Processing*, 25(4):331–351, 2011.
6. S. Formentin, K. Heusden, and A. Karimi. A comparison of model-based and data-driven controller tuning. *International Journal of Adaptive Control and Signal Processing*, 28(10):882–897, 2014.

7. L. Campestrini, M. Gevers, and A.S. Bazanella. Virtual Reference Feedback Tuning for Non Minimum Phase Plants. In *European Control Conference (ECC 2009), Budapest, Hungary, pp. 1955-1960*, 2009.
8. S. Formentin, M. Corno, S.M. Savaresi, and L. Del Re. Direct data-driven control of linear time-delay systems. *Asian Journal of Control*, 13(5):1–12, 2011.
9. S. Formentin and A. Karimi. Enhancing statistical performance of data-driven controller tuning via L_2-regularization. *Automatica*, 50(5):1514–1520, 2014.
10. F. Previdi, T. Schauer, S.M. Savaresi, and K.J. Hunt. Data-driven control design for neuroprotheses: a virtual reference feedback tuning (VRFT) approach. *IEEE Transactions on Control Systems Technology*, 12(1):176–182, 2004.
11. S. Formentin, M.C. Campi, and S.M. Savaresi. Virtual reference feedback tuning for industrial PID controllers. In *19th IFAC World Congress, Cape Town, South Africa*, pages 11275–11280, 2014.
12. P. Panizza, D. Invernizzi, F. Riccardi, S. Formentin, and M. Lovera. Data-driven attitude control law design for a variable-pitch quadrotor. In *2016 American Control Conference (ACC)*, pages 4434–4439, 2016.
13. F. Riccardi and M. Lovera. Robust attitude control for a variable-pitch quadrotor. In *IEEE Conference on Control Applications, Antibes, France*, pages 730–735, 2014.
14. S. Formentin, A. Cologni, D. Belloli, F. Previdi, and S.M. Savaresi. Fast tuning of cascade control systems. In *18th IFAC World Congress, Milan, Italy*, pages 10243–10248, 2011.
15. S. Capocchiano, P. Panizza, D. Invernizzi, and M. Lovera. Closed-loop data-driven attitude control design for a multirotor uav. In *2018 IEEE Conference on Control Technology and Applications (CCTA)*, pages 153–158, 2018.
16. S. Formentin, S.M. Savaresi, and L. Del Re. Non-iterative direct data-driven controller tuning for multivariable systems: theory and application. *IET control theory & applications*, 6(9):1250–1257, 2012.
17. D. Invernizzi, P. Panizza, F. Riccardi, S. Formentin, and M. Lovera. Data-driven attitude control law of a variable-pitch quadrotor: a comparison study. *IFAC-PapersOnLine*, 49(17):236 – 241, 2016. 20th IFAC Symposium on Automatic Control in Aerospace 2016.
18. T. Söderström and P. Stoica. Instrumental variable methods for system identification. *Circuits, Systems and Signal Processing*, 21(1):1–9, 2002.
19. Lucíola Campestrini, Diego Eckhard, Lydia Andrea Chía, and Emerson Boeira. Unbiased mimo vrft with application to process control. *Journal of Process Control*, 39:35–49, 2016.
20. M. Nakamoto. An application of the virtual reference feedback tuning for an MIMO process. In *SICE 2004 Annual Conference*, volume 3, pages 2208–2213 vol. 3, 2004.
21. S. Formentin, A. Bisoffi, T. Oomen. Asymptotically exact direct data-driven multivariable controller tuning. *IFAC-PapersOnLine*, 48(28):1349 – 1354, 2015. 17th IFAC Symposium on System Identification SYSID 2015.
22. D. Selvi, D. Piga, and A. Bemporad. Towards direct data-driven model-free design of optimal controllers. In *2018 European Control Conference (ECC)*, pages 2836–2841, 2018.

23. G. R. Gonçalves da Silva, A. S. Bazanella, and L. Campestrini. On the choice of an appropriate reference model for control of multivariable plants. *IEEE Transactions on Control Systems Technology*, 27(5):1937–1949, 2019.